The role of nearest neighbour anharmonic couplings in the phase diagram of betaine calcium chloride dihydrate (BCCD)

1999 J. Phys.: Condens. Matter 11 5497

(http://iopscience.iop.org/0953-8984/11/28/310)

J. Phys.: Condens. Matter **11** (1999) 5497–5504. Printed in the UK PII: S0953-8984(99)99970-8

The role of nearest neighbour anharmonic couplings in the phase diagram of betaine calcium chloride dihydrate (BCCD)

I Etxebarria†, J Hlinka‡ and M Quilichini§

† Fisika Aplikatua II Saila, Zientzi Fakultatea, Euskal Herriko Unibertsitatea, PK 644, 48080 Bilbo, Spain
‡ Institute of Physics, Academy of Science of the Czech Republic, Na Slovance 2, CZ-18040 Praha 8, Czech Republic
§ Laboratoire Léon Brillouin, Centre d'Etudes de Saclay, 91191 Gif-sur-Yvette Cédex, France

E-mail: wmpetali@lg.ehu.es (I Etxebarria)

Received 4 December 1998, in final form 8 April 1999

Abstract. We present the results of mean-field calculations on a symmetry based semimicroscopic model for betaine calcium chloride dihydrate. The model takes into account the three degrees of freedom associated with the lowest energy phonon branches as relevant variables and experimental inelastic neutron scattering data and observed transition temperatures are used to fit the coupling constants of the model potential. Although the method does not allow us to predict incommensurate phases, the results show the failure of previous models based on continuous variables to reproduce the observed phase diagram. The insertion of a new term in the model potential corresponding to anharmonic interactions between nearest neighbours is shown to be crucial to stabilize some experimentally observed commensurate phases.

1. Introduction

Betaine calcium chloride dihydrate (BCCD) exhibits a very rich sequence of phase transitions [1–3] corresponding to different commensurate and incommensurate phases modulated along the c axis. At room temperature the crystal is orthorhombic with space group *Pnma*. At 164 K the structure becomes modulated with an incommensurate wavevector close to $\boldsymbol{k} = \frac{1}{3}\boldsymbol{c}^*$ and at lower temperatures the modulation wavevector decreases monotonically down to $\boldsymbol{k} = 0$ at 46 K. Between these temperatures BCCD presents a great variety of high order commensurate and incommensurate phases resembling a devil's staircase behaviour (see [4] and [5] for reviews about the experimental and theoretical results respectively). Another striking feature of BCCD is its sensitivity to external fields. Changes of pressure and electric field affect considerably the stability range of the observed phases [6, 7].

Landau theory has been often used to study modulated crystals, but, as for each commensurate phase a different lock-in term must be included in the free energy expansion, the presence of a large number of commensurate phases in the case of BCCD makes this kind of approach rather artificial [8, 9]. Nevertheless, a symmetry analysis [10] of the phase transitions in BCCD shows that the symmetry of the order parameter may be the same for the whole sequence of phase transitions. The successive transitions take place through the lock-in of the wavevector into different commensurate values [11] but the symmetry transformation properties of the order parameter are not altered.

0953-8984/99/285497+08$30.00

Two different microscopic approaches have been used in the literature to explain the existence of complex phase diagrams including commensurate and incommensurate phases like that of BCCD. On one hand, if the spatial range of the interactions between the basic degrees of freedom of the model is extended to further neighbours, the instabilities may lie at a general point in the Brillouin zone and give rise to incommensurate phase transitions [12, 13]. On the other hand, if the interactions are limited to nearest neighbours but the number of degrees of freedom per cell is increased a similar behaviour may be obtained [14]. This second point of view can be easily be interpreted in terms of the dynamics of the system, the interaction between the phonon branches associated with the relevant degrees of freedom being the origin of the instability [15]. In fact, the same mechanism applies to the double Ising spin (DIS) wich has been used as a frame for interpretation of the phase diagram of BCCD in several recent papers [16–18]. However, as the main ingredients of the DIS model are pseudo-spin variables, relation to the soft phonon dynamics observed in experiments is lost.

Inelastic neutron scattering measurements in the high temperature phase [19] of BCCD show that the three lowest energy branches interact strongly and this interaction seems to be the origin of the critical mode that destabilizes the structure. According to [10] the frozen combination of the three degrees of freedom corresponding to the three branches should be almost the same for all the modulated phases, only the amplitude and the lock-in global phase could vary to give the symmetries observed experimentally. This point of view has been exploited to obtain two models [20, 21] based on two continuous variables per half cell. Hlinka *et al* [20] calculated the thermal renormalization of the harmonic couplings due to the anharmonic terms of the Hamiltonian by fitting the temperature dependence of the experimental phonon branches but no further analysis of the phase diagram is done. Kappler and Walker [21] proposed a symmetry-adapted free energy and studied the stability range of the commensurate phases. Thermal effects were supposed to affect in an effective manner the harmonic terms of the free energy and the path in the parameter space that corresponds to the experimental phase transitions was obtained varying *ad hoc* the harmonic couplings with temperature.

In this work these two previous models are revised and extended. The values of all the couplings are calculated from the experimental phonon branches in the high temperature phase [19] and the transition temperatures between several observed structures. Once the parameters are obtained the resulting phase diagram is studied and compared with the experimental one. All the calculations have been done within the mean-field approximation and only low-order commensurate phases have been included in the phase diagrams.

2. The model

The structure of BCCD in the normal phase is orthorhombic with space group *Pnma* and four structural units per unit cell. According to [20] the structure may be simplified considering the four columns along the b axis composed by the betaine molecules and the neighbouring inorganic Ca complexes (see figures 1, 2 and 3 of [20]). The rotations of both betaine and Ca complexes along their preferential axis in the (a, c) plane are known to be strongly correlated within one column in the *Pnma* phase [20]. An analysis of the modulated phases shows that this correlation is also present in the frozen distortions of some commensurate and incommensurate structures of BCCD [22]. Considering that this correlation is infinitely strong, the four librational degrees of freedom associated with each column in the unit cell give rise to two optic branches in a extended zone scheme. The uniform translations of the columns along the b axis correspond to two more branches one of them being the acoustic one. As we are mainly interested in the dispersion branches along the c^* direction, columns at different cells lying at the same c coordinate are supposed to be also completely correlated and we need just

one index to describe the distortions of the whole layers of columns perpendicular to c: x_n and y_n for the displacements and η_n and ξ_n for the librations. Under these assumptions the glide plane σ_a operates on the four variables as a translation $c/2$, thus, the phonon eigenvectors can be defined in one half of the unit cell and the Brillouin zone is doubled. The periodicity of the model crystal is $c/2$ with four variables per reduced cell.

The model potential can be expressed as [20]

$$\begin{aligned} V = \sum_i [&a_1(x_i^2 + y_i^2) + a_2 x_i y_i + a_3(x_i x_{i+1} + y_i y_{i+1}) + a_4(\eta_i^2 + \xi_i^2) + a_5\eta_i\xi_{i+1} + a_6\eta_i\xi_i \\ &+a_7(\eta_i\eta_{i+1} + \xi_i\xi_{i+1}) + a_8\eta_{i+1}\xi_i + a_9(\xi_i x_i + \eta_i y_i) + a_{10}(\xi_i y_i + \eta_i x_i) \\ &+a_{11}(x_i\xi_{i+1} + \eta_i y_{i+1}) + a_{12}(x_{i+1}\xi_i + \eta_{i+1} y_i) + b_1(\eta_i^4 + \xi_i^4) \\ &+b_2\eta_i^2\xi_i^2 + b_3\xi_i\eta_i(\eta_i^2 + \xi_i^2)]. \end{aligned} \tag{1}$$

The last three terms represent the only symmetry allowed anharmonic interactions that involve rotations in the same layer.

Phonons propagating along c^* may be constructed from the following linear combination of the relevant variables:

$$\phi_i = \frac{\xi_i + \eta_i}{\sqrt{2}} \qquad \psi_i = \frac{\xi_i - \eta_i}{\sqrt{2}} \qquad u_i = \frac{x_i + y_i}{\sqrt{2}} \qquad v_i = \frac{x_i - y_i}{\sqrt{2}}.$$

The Fourier transform of these symmetry adapted variables may be interpreted as the collective displacement coordinates that correspond to the following representations at $k = 0$ and $k = c^*$ [20, 21]:

$$\begin{aligned} &\phi(k=0) \text{ and } u(k=0) \to \mathrm{B}_{2u} \qquad &&\phi(k=c^*) \text{ and } u(k=c^*) \to \mathrm{B}_{1g} \\ &\psi(k=0) \text{ and } v(k=0) \to \mathrm{B}_{3g} \qquad &&\psi(k=c^*) \text{ and } v(k=c^*) \to \mathrm{A}_u. \end{aligned}$$

In the present work a further simplification will be assumed. As the fourth branch in the experimental phonon curves lies at quite high energies it does not mix significantly with the two librational branches and it does not seem to play an essential role in the phase transition mechanism. So, the antisymmetric displacement coordinate v_i has been dropped and the potential in the new basis becomes

$$\begin{aligned} V = \sum_i \Bigg[&\frac{A_1}{8}(u_i - u_{i+1})^2 + \frac{A_2}{2}\phi_i^2 + \frac{A_3}{2}\psi_i^2 + \frac{A_4}{2}\phi_i\phi_{i+1} + \frac{A_5}{2}\psi_i\psi_{i+1} \\ &+\frac{A_6}{4}u_i(2\phi_i - \phi_{i+1} - \phi_{i-1}) + \frac{A_7}{2}u_i(\psi_{i+1} - \psi_{i-1}) + \frac{A_8}{2}\phi_i(\psi_{i+1} - \psi_{i-1}) \\ &+\frac{B_1}{4}\phi_i^4 + \frac{B_2}{4}\psi_i^4 + \frac{B_3}{4}\phi_i^2\psi_i^2 \Bigg]. \end{aligned} \tag{2}$$

The corresponding dynamical matrix may be written as

$$D(k) = \begin{bmatrix} A_1 \sin^2\dfrac{k\pi}{2} & A_6 \sin^2\dfrac{k\pi}{2} & \mathrm{i}A_7 \sin k\pi \\ A_6 \sin^2\dfrac{k\pi}{2} & A_2 + A_4\cos k\pi & \mathrm{i}A_8 \sin k\pi \\ -\mathrm{i}A_7 \sin k\pi & -\mathrm{i}A_8 \sin k\pi & A_3 + A_5 \cos k\pi \end{bmatrix}. \tag{3}$$

It has to be pointed out that the model potential (2) and the dynamical matrix (3) correspond to the model [21], apart from the explicit treatment of the thermal renormalization that will be explained in the next section.

The number of unknown coefficients may be reduced using some experimental results. From ultrasound experiments [23] and the observed slope of the acoustic branch [19] we have

$A_1 = 1.8 \times 4\pi^2$ THz^2. At low temperatures, the frequency of the two soft optic phonon branches increases and the saturated value of the lowest frequency at $k = 0$ is around 1.0 THz [24, 25]. At $T = 0$ this corresponds to the condition $\sqrt{2(A_2 - A_4)} = 1 \times 4\pi^2$ THz^2. Using these two restrictions the number of parameters to be obtained is eight, five harmonic couplings and three anharmonic ones.

3. Mean-field approximation

3.1. Structures and free energy

The eight model parameters have been obtained from information about the experimental phonon branches at different temperatures and some transition temperatures between selected commensurate phases. Thus, the core of the fitting procedure requires us to obtain the renormalizing effect of the anharmonic terms over the vibrational frequencies and the free energies of equilibrium structures for a given periodicity.

In the independent-site approximation [13] the effect of the neighbours is taken into account as an average field and the variables at site i 'feel' the following potential:

$$\begin{aligned} V_i = {} & \frac{A_1}{4}u_i(u_i - \bar{u}_{i-1} - \bar{u}_{i+1}) + \frac{A_2}{2}\phi_i^2 + \frac{A_3}{2}\psi_i^2 + \frac{A_4}{2}\phi_i(\bar{\phi}_{i+1} + \bar{\phi}_{i-1}) \\ & + \frac{A_5}{2}\psi_i(\bar{\psi}_{i+1} + \bar{\psi}_{i-1}) + \frac{A_6}{4}[2u_i\phi_i - u_i(\bar{\phi}_{i+1} + \phi_{i-1}) - \phi_i(\bar{u}_{i+1} + \bar{u}_{i-1})] \\ & + \frac{A_7}{2}[u_i(\bar{\psi}_{i+1} - \bar{\psi}_{i-1}) + \psi_i(\bar{u}_{i-1} - \bar{u}_{i+1})] \\ & + \frac{A_8}{2}[\phi_i(\bar{\psi}_{i+1} - \bar{\psi}_{i-1}) + \psi_i(\bar{\phi}_{i-1} - \bar{\phi}_{i+1})] + \frac{B_1}{4}\phi_i^4 + \frac{B_2}{4}\psi_i^4 + \frac{B_3}{4}\phi_i^2\psi_i^2 \end{aligned} \tag{4}$$

and the mean values are calculated selfconsistently:

$$\bar{\chi}_i = \frac{1}{Z_i}\int \chi \exp\left(\frac{V_i}{T}\right) \mathrm{d}u\, \mathrm{d}\phi\, \mathrm{d}\psi \qquad \chi = u, \phi, \psi$$
$$\text{with } Z_i = \int \exp\left(-\frac{V_i}{T}\right) \mathrm{d}u\, \mathrm{d}\phi\, \mathrm{d}\psi. \tag{5}$$

The entropy may be written as

$$S = \sum_i S_i = -\sum_i \int w_i(u, \phi, \psi) \ln w_i(u, \phi, \psi)\, \mathrm{d}u\, \mathrm{d}\phi\, \mathrm{d}\psi$$
$$\text{with } w_i(u, \phi, \psi) = \frac{1}{Z_i}\exp\left(-\frac{V_i}{T}\right)$$

and the free energy becomes [13]:

$$\begin{aligned} F = -\sum_i \Bigg[& -\frac{A_1}{4}\bar{u}_i\bar{u}_{i+1} + A_4\bar{\phi}_i\bar{\phi}_{i+1} + A_5\bar{\psi}_i\bar{\psi}_{i+1} - \frac{A_6}{4}\bar{u}_i(\bar{\phi}_{i+1} + \bar{\phi}_{i-1}) \\ & + \frac{A_7}{4}\bar{u}_i(\bar{\psi}_{i+1} - \bar{\psi}_{i-1}) + \frac{A_8}{4}\bar{\phi}_i(\bar{\psi}_{i+1} - \bar{\psi}_{i-1}) + T\ln Z_i \Bigg]. \end{aligned} \tag{6}$$

Thus, for an n/m commensurate structure there are $6m$ equations (equation (5)) to be solved selfconsistently in order to obtain the equilibrium structure and the corresponding free energy.

3.2. Phonons

The calculation of phonon branches requires us to go beyond the mean-field theory to take into account the fluctuations [13]. The effect of the temperature arises from the on-site potential, the couplings between adjacent variables being treated exactly. In the high temperature phase the mean value of the three variables is zero and the on-site potential (4) becomes:

$$V_i = \frac{A_1}{4}u_i^2 + \frac{A_2}{2}\phi_i^2 + \frac{A_3}{2}\psi_i^2 + \frac{A_6}{2}u_i\phi_i + \frac{B_1}{4}\phi_i^4 + \frac{B_2}{4}\psi_i^4 + \frac{B_3}{4}\phi_i^2\psi_i^2$$

that can be approximated by a harmonic potential:

$$V_i^{HAR} = \frac{A_1}{4}u_i^2 + \frac{A_2^*(T)}{2}\phi_i^2 + \frac{A_3^*(T)}{2}\psi_i^2 + \frac{A_6}{2}u_i\phi_i$$

where $A_2^*(T)$ and $A_3^*(T)$ must be calculated to ensure that the on-site potential and its harmonic approximation give the same value of the fluctuations at a given temperature. For the harmonic potential we have:

$$\langle\phi^2\rangle_{HAR} = \frac{2A_1}{2A_1A_2^*(T) - A_6^2}T \qquad \text{and} \qquad \langle\psi^2\rangle_{HAR} = \frac{T}{A_3(T)}.$$

Thus, both potentials give the same fluctuations if the harmonic couplings are chosen in the following way:

$$A_2^*(T) = \frac{A_6^2\overline{\phi^2} + 2A_1T}{2A_1\overline{\phi^2}} \qquad A_3^*(T) = \frac{T}{\overline{\psi^2}} \tag{7}$$

where $\overline{\phi^2}$ and $\overline{\psi^2}$ represent the fluctuations calculated numerically with the anharmonic potential.

Thus, the values of $\overline{\phi^2}$ and $\overline{\psi^2}$ give us the renormalized coefficients $A_2^*(T)$ and $A_3^*(T)$ that have to be used instead of A_2 and A_3 in the expression of the dynamical matrix (3) to take into account the thermal renormalization of the phonon branches.

4. Results

Inelastic neutron scattering measurements performed in the high temperature phase [20] and information about transition temperatures between some commensurate phases provide enough information to fit all the potential parameters. The eigenvalues of the dynamical matrix were calculated at four different temperatures, 164, 170, 190 and 250 K. The first contribution to the least square fitting corresponds to the differences between the calculated and experimental frequencies (93 values) and two additional conditions for the frequency of the soft mode, $\mathrm{d}\omega/\mathrm{d}k = 0$ and $\omega = 0$ at $\boldsymbol{k} = 0.32\ \boldsymbol{c}^*$ and $T_1 = 164$ K. The experimental transition temperatures were taken into account calculating the free energy of the $1/4_{II}$, $1/5_{II}$, $1/7_{II}$ and $0/1_{II}$ phases and the following conditions were added to the least squares fitting:

$$F_{\frac{1}{4_{II}}}(75\text{ K}) = F_{\frac{1}{5_{II}}}(75\text{ K}) \qquad F_{\frac{1}{7_{II}}}(46\text{ K}) = F_{\frac{0}{1_{II}}}(46\text{ K}) \tag{8}$$

where F represents the free energy of the equilibrium structure. Due to correlations between the anharmonic parameters similar values of the goodness of the fit were obtained for parameter sets corresponding to quite different phase diagrams. Thus, we decided to perform different fits for a fixed value of the B_3 anharmonic parameter. For each value of B_3 the parameter set that gives the best fit has been used to calculate the free energies of the n/m commensurate phases with $n \leqslant 2$ and $m \leqslant 7$. The global phase of the modulation was obtained by looking at the position of the maxima, minima and zeros of the obtained profiles for $\overline{u_i}$, $\overline{\phi_i}$ and

Table 1. Possible space groups of the commensurate phases of BCCD considering an unique symmetry of the order parameter (Λ_3) for different wavevectors ($\boldsymbol{k} = (n/m)\boldsymbol{c}^*$) and global phases of the modulation (Φ) [10].

n/m	Label	Φ	Space group
odd/odd	I	0	$P112_1/a$
	II	$\pi/2$	$P2_12_12_1$
	III	arbitr.	$P112_1$
even/odd	I	0	$P2_1/n11$
	II	$\pi/2$	$Pn2_1a$
	III	arbitr.	$Pn11$
odd/even	I	0	$P12_1/c1$
	II	$(n/2m)\pi$	$P2_1ca$
	III	arbitr.	$P1c1$

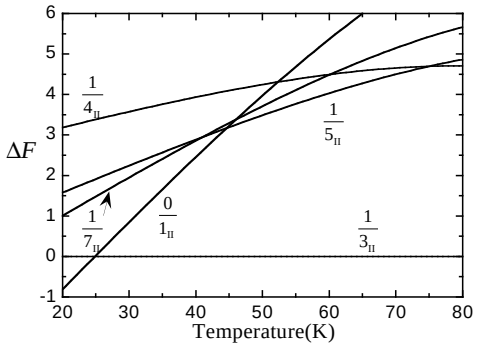

Figure 1. Free energy ($\Delta F(\times 4\pi^2 \times 10^3$ THz^2)) of the $1/4_{II}$, $1/5_{II}$, $1/7_{II}$ and $0/1_{II}$ phases with respect to the $1/3_{II}$ phase for the model potential without nearest neighbour anharmonic interactions. The model parameters were fitted using the experimental phonon branches and two transition temperatures between commensurate phases ($B_3 = 0.08 \times 4\pi^2$ THz^2).

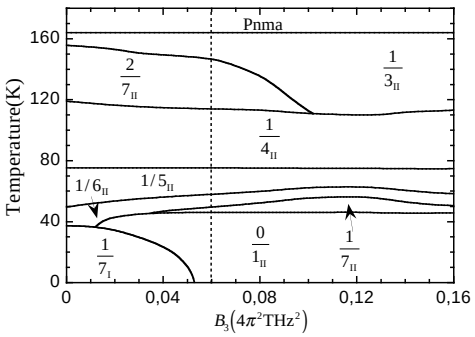

Figure 2. Phase diagram obtained by fitting the model parameters using the experimental phonon branches and two transition temperatures for the model including nearest neighbour anharmonic interactions. The dashed line at $B_3 = 0.06 \times 4\pi^2$ THz^2 indicates a phase transition sequence similar to that observed in BCCD.

$\overline{\psi_i}$ after solving the selfconsistency equations (5) and in all cases the obtained structures were of type I and II (see table 1). The results show that at low and high values of B_3 the ground states correspond to the $1/2_I$ and $1/2_{II}$ phases respectively. For a small range of $B_3(0.06 \times 4\pi^2$ THz$^2 < B_3 < 0.13 \times 4\pi^2$ THz$^2)$ the low temperature phase agrees with the experimentally observed ferroelectric $0/1_{II}$ phase but the high order commensurate phases are not stable in any temperature range. In figure 1 the free energies of the various phases are represented for $B_3 = 0.08 \times 4\pi^2$ THz^2 in comparison with the free energy of the $1/3_{II}$ phase ($\Delta F = F_\alpha - F_{\frac{1}{3_{II}}}$). Although the condition (8) is fulfilled, the low values of the free energy of the $1/3_{II}$ phase prevent the stabilization of the high order phases and a direct transition from the $1/3_{II}$ phase to the $0/1_{II}$ is obtained at 25 K.

Some further attempts to improve the model were made by introducing new harmonic couplings of longer range but the results did not change significantly. However, the insertion of anharmonic couplings between adjacent layers changed drastically the resulting phase diagram.

One of the possible terms to be considered is [20]

$$\frac{B_4}{4}(\xi_i^2\xi_{i+1}^2 + \eta_i^2\eta_{i+1}^2) \tag{9}$$

which in terms of the symmetry adapted variables becomes

$$\frac{B_4}{4}[\phi_i^2\phi_{i+1}^2 + \psi_i^2\psi_{i+1}^2 + \phi_i^2\psi_{i+1}^2 + \phi_{i+1}\psi_1^2 + 4\phi_i\psi_i\phi_{i+1}\psi_{i+1}].$$

The insertion of this interaction implies the addition of the following term to the on-site potential in equation (4):

$$\frac{B_4}{4}[(\phi_i^2 + \psi_i^2)(\overline{\phi_{i+1}^2} + \overline{\phi_{i-1}^2} + \overline{\psi_{i+1}^2} + \overline{\psi_{i-1}^2}) + 4\phi_i\psi_i(\overline{\phi_{i+1}\psi_{i+1}} + \overline{\phi_{i-1}\psi_{i-1}})].$$

This term modifies the calculation of the phonon frequencies and equilibrium structures. On one hand, as $\overline{\phi_i^2}$ and $\overline{\psi_i^2}$ are not null in the *Pnam* phase the calculation of the parameters of the harmonic approximation (equation (7)) in the high temperature phase to obtain the phonon branches becomes a selfconsistency problem. On the other hand, the mean-field calculation of the structure (equation (5)) requires not only selfconsistency on the mean values $\bar{u}_i$, $\bar{\phi}_i$ and $\bar{\psi}_i$, but also in the correlation terms $\overline{\phi_i^2}$, $\overline{\psi_i^2}$ and $\overline{\phi_i\psi_i}$, so six variables for each layer.

The model parameters were obtained as in the previous model, that is, for different values of B_3 the rest of the model parameters were fitted using the experimental information about the phonon branches and the two transition temperatures between commensurate phases at 75 and 46 K. The inclusion of the new anharmonic term improved the goodness of fit and changed drastically the phase diagram as can be seen in figure 2. For small values of B_3 the ground state does not correspond to the observed $0/1_{II}$ phase and at high values the $2/7_{II}$ phase disappears. In the central region the phase diagram resembles qualitatively that of BCCD. In table 2 the obtained model parameters and transition temperatures for $B_3 = 0.06 \times 4\pi$ THz^2 are listed. The agreement with the experimental values is quite good and shows the ability of this model to reproduce correctly the observed sequence of phase transitions in BCCD at zero pressure. Since the model contains three relevant degrees of freedom, nearest neighbour harmonic interactions are sufficient for the presence of incommensurate phases [14]. Thus, the existence of the $1/3_{II}$ phase has to be interpreted within the limits of the present calculations. We have obtained that at high temperatures the energy of the tripled phase is lower than that of the $2/7_{II}$ phase but this does not exclude incommensurate phases being stable at these temperatures. The calculation of the range of stability of the incommensurate and high order commensurate phases would require more sophisticated methods such as fixed point expansions [16] which are out of the scope of this work.

Table 2. Model parameters ($\times 4\pi^2$ THz^2) and phase transition sequence for the model with nearest neighbour anharmonic coupling and $B_3 = 0.06 \times 4\pi^2$ THz^2.

$A_1 = 1.8$	$A_2 = -0.2387$	$A_3 = 0.0732$	$A_4 = -0.2613$	$A_5 = 0.1319$	$A_6 = -0.3741$
$A_7 = 0.2065$	$A_8 = 0.1557$	$B_1 = 0.068\,86$	$B_2 = 0.019\,13$	$B_4 = -0.014\,60$	

$$Pnma \xrightarrow[164.0\text{ K}]{} \frac{1}{3_{II}} \xrightarrow[146.9\text{ K}]{} \frac{2}{7_{II}} \xrightarrow[113.9\text{ K}]{} \frac{1}{4_{II}} \xrightarrow[75.2\text{ K}]{} \frac{1}{5_{II}} \xrightarrow[57.9\text{ K}]{} \frac{1}{6_{II}} \xrightarrow[49.6\text{ K}]{} \frac{1}{7_{II}} \xrightarrow[46.1\text{ K}]{} \frac{0}{1_{II}}$$

5. Conclusions

The anharmonic interaction between nearest neighbours plays a fundamental role in the behaviour of models for BCCD based on continuous variables. In a rigorous treatment, this interaction should produce the thermal renormalization of the dispersion of the bare branches,

that is, the temperature dependence of the coupling parameters A_4 and A_5. In the present work, within the mean-field approximation, the dispersion of the bare branches is kept constant. The presence of the anharmonic coupling between nearest neighbours changes the values of the rest of the anharmonic couplings, equilibrium structures at a given temperature and associated energies, this change being essential to obtain a phase diagram in agreement with the observed behaviour of BCCD.

Some remarks may be made in relation to the results presented by Kappler and Walker [21]. They reproduce the experimental phase sequence by varying *ad hoc* two linear combinations of the harmonic couplings in their symmetry-adapted free energy. Actually the critical parameter that influences more drastically the behaviour of their model corresponds to the sum $J_+ = A_4 + A_5$ and the variation of this parameter is necessary to reproduce the correct phase diagram. The temperature variation of the J_+ coefficient corresponds to a renormalization of the dispersion of the two bare optic branches. As mentioned, the last term (8) added to our potential produces the same kind of renormalization, so it may be concluded that the importance of nearest neighbour anharmonic interactions to stabilize the high order phases is implicitly present in [21]. The anharmonic coupling between adjacent layers produces changes of the dispersion of the bare optic branches with temperature and this thermal effect is the one that gives the correct path in the phase diagram.

Acknowledgments

One of the authors (IE) expresses his gratitude for the warm hospitality during his stay at LLB and the financial support of the 'Human Capital and Mobility' program of the European Union. This work was also partially supported by the Basque Government (project PI97-71).

References

[1] Rother H J, Albers J and Klöpperpieper A 1984 *Ferroelectrics* **54** 107
[2] Brill W and Ehses K H 1985 *Japan. J. Appl. Phys.* **24** 826
[3] Klöpperpieper A, Brill W and Ehses K H 1985 *Japan. J. Appl. Phys.* **24** 826
[4] Schaack G and Le Maire M 1998 *Ferroelectrics* **208** 1
[5] Neubert B, Pleimling M and Siems R 1998 *Ferroelectrics* **208** 141
[6] Ao R, Schaack G, Schmitt M and Zöller M 1989 *Phys. Rev. Lett.* **62** 183
[7] Le Maire M, Straub R and Schaack G 1997 *Phys. Rev.* B **56** 134
[8] Ribeiro J L, Tolédano J C, Chaves M R, Almeida A, Müser H E, Albers J and Klöpperpieper A 1990 *Phys. Rev.* B **41** 2343
[9] Sannikov D G and Schaack G 1998 *J. Phys.: Condens. Matter* **10** 1803
[10] Perez-Mato J M 1988 *Solid State Commun.* **67** 1145
[11] Ezpeleta J M, Zuñiga F J, Paulus W, Cousson A, Hlinka J and Quilichini M 1996 *Acta Crystallogr.* B **52** 810
[12] Selke W 1988 *Phys. Rep.* **170** 213
[13] Janssen T and Tjon J A 1983 *J. Phys. C: Solid State Phys.* **16** 4789
[14] Janssen T 1992 *Z. Phys.* B **86** 277
[15] Etxebarria I, Quilichini M, Perez-Mato J M, Boutroille P, Zuñiga F J and Breczewski T 1992 *J. Phys.: Condens. Matter* **4** 8551
[16] Pleimling M and Siems R 1994 *Ferroelectrics* **151** 69
[17] Pleimling M and Siems R 1996 *Ferroelectrics* **185** 103
[18] Neubert B, Pleimling M, Tentrup Th and Siems R 1994 *Ferroelectrics* **155** 359
[19] Hlinka J, Quilichini M, Currat R and Legrand J F 1996 *J. Phys.: Condens. Matter* **8** 8207
[20] Hlinka J, Quilichini M, Currat R and Legrand J F 1996 *J. Phys.: Condens. Matter* **8** 8221
[21] Kappler C and Walker M B 1993 *Phys. Rev.* B **48** 5902
[22] Hlinka J 1995 *PhD Thesis* Paris
[23] Haussühl S, Liedtke J, Albers J and Klöpperpieper A 1988 *Z. Phys.* B **70** 219
[24] Kamba S, Petzelt J, Dvořák V, Goncharov Yu G, Volkov A A, Kozlov G V and Albers J 1990 *Ferroelectrics* **105** 351
[25] Hlinka J, Hernandez O, Quilichini M and Currat R 1996 *Ferroelectrics* **185** 221